

CO₂ release in vertical tube falling film evaporators

Jan-Helge Donner^a, Jürren Fokken^b, Katharina Boeck^a,
Heike Glade^{a*}, Stefan Will^a

^aUniversität Bremen, Technische Thermodynamik, Badgasteiner Str. 1, D-28359 Bremen, Germany
Tel. +49 421 2182443; Fax +49 421 2187555; email: heike.glade@uni-bremen.de

^bPresent address: Nordostschweizerische Kraftwerke AG, Döttingen, Switzerland

Received 15 March 2007; accepted 15 April 2007

Abstract

The release of non-condensable (NC) gases, essentially carbon dioxide, oxygen and nitrogen, from the evaporating brine in desalination distillers notably affects the heat transfer for condensation, the energy consumption, the performance and the material life span of the distillers. A better knowledge of CO₂ release and of the interaction with the carbonate system in desalination distillers is very important for the design of the venting system and a stable distiller operation. Since CO₂ release and scale formation are closely related to the carbonate system of the brine, a better understanding of CO₂ release may contribute to the knowledge of scale formation in desalination distillers and improve scale prediction and prevention methods.

A model has been developed for the prediction of the CO₂ release rates in falling film evaporators with vertical tubes. The theory of mass transfer coupled with chemical reaction kinetics (chemical desorption) was applied to the problem of CO₂ release. The mass transfer and the chemical reaction kinetics were studied for the conditions prevailing in falling film seawater evaporators. In addition to the CO₂ release rates the model allows for calculation of the HCO₃⁻, CO₃²⁻, CO₂, H⁺, and OH⁻ concentrations in the carbonate system of the brine. The model was applied to a falling film evaporator at various operating conditions. The release rates of CO₂ along the flow path of the falling film were determined.

The paper presents the main principles of the model and discusses the simulation results. The effects of process parameters and the seawater properties such as evaporation temperature, seawater salinity, and pH value on the CO₂ release rates are shown. Moreover, the paper discusses in which desorption regime (e.g. slow, fast, instantaneous) the CO₂ release process takes place and whether the mass transfer is enhanced by the chemical reactions.

Keywords: CO₂ release; Carbonate system; Vertical tube falling film; Modeling; Simulation

*Corresponding author.

Presented at the conference on Desalination and the Environment. Sponsored by the European Desalination Society and Center for Research and Technology Hellas (CERTH), Sani Resort, Halkidiki, Greece, April 22–25, 2007.

1. Introduction

In falling film evaporators liquid is fed to the top of a vertical tube bundle, flows down the inner walls as a thin film under gravity and evaporates from the surface. Steam condenses on the outside of the tubes supplying the energy required.

Vertical tube falling film evaporators were used in the first desalination plants. As the capacity of desalination plants became bigger, falling film evaporators — because of their susceptibility to scale formation — were replaced by multi-stage flash (MSF) plants. Nowadays, the interest in vertical tube falling film evaporators is being revived (e.g. [1]).

Non-condensable (NC) gases, essentially carbon dioxide, nitrogen, and oxygen, cause serious problems in the condensers of desalination systems. They are responsible for a significant reduction of the overall heat transfer coefficient and hence for a lower performance of desalination plants. The pH value of the condensate is lowered by dissolving CO_2 . In conjunction with the presence of oxygen this effect may lead to corrosion of the condenser tubes. Furthermore, the release of carbon dioxide notably influences the concentrations of the components in the carbonate system of the brine, which is important for alkaline scale formation. Therefore, it is necessary to remove NC gases from the condensers by adequate venting. Knowledge on NC gases is important for a proper design of the venting systems so that their energy consumption is as low as possible. In addition, a better understanding of CO_2 release is useful for prediction of scale formation.

2. Desorption with and without chemical reaction

The desorption of a dissolved gas from a liquid into an adjacent gaseous phase will take place if the concentration of the gas in the bulk of the liquid is higher than that at the phase interface. The desorption of a gas from a liquid can be caused by reducing the total pressure or the partial pressure

of the gas, by increasing the temperature of the solution or the ionic strength or by chemical reactions within the solution [2]. Desorption can be subdivided into chemical and physical desorption. If the desorption takes place with chemical reactions between the dissolved gas and the components of the solution, the desorption is called “chemical desorption”. Otherwise the desorption is called “physical desorption” [2,3]. While the release of nitrogen, oxygen, and argon from seawater can be treated as a problem of physical desorption, the theory of chemical desorption has to be applied to the problem of carbon dioxide release from the evaporating brine in desalination distillers.

In desorption processes the occurrence of chemical reactions can have two distinct effects on mass transfer [3–6]. Chemical reactions provide a certain concentration of the molecularly dissolved gas in the bulk of the liquid and hence a certain driving force for the mass transfer. At a given level of driving force, the actual rate of mass transfer may be significantly larger when chemical reactions are taking place than it would be in the absence of chemical reactions. Depending on the relative rates of the reactions and the mass transfer, the desorption may take place in different regimes: the slow reaction regime subdivided into the kinetic and the diffusional regime, the fast reaction regime, and the instantaneous reaction regime. In addition to these asymptotic cases, transition regions are known to occur. In the fast and instantaneous reaction regime the reaction may significantly enhance the mass transfer.

There are two mechanisms of gas desorption from aqueous solutions. If the difference between the partial pressure of the gas in equilibrium with the bulk liquid and the partial pressure at the surface, i.e., the degree of supersaturation, is modest, the gas will be desorbed by quiescent desorption [7,8]. However, if the degree of supersaturation is large, bubbles will form in the interior of the liquid and much of the gas will be released by diffusing from the surface of the

bubbles (bubble desorption). Thus, bubble desorption is a process very different from quiescent desorption and absorption processes in which the area of surface available for mass transfer is determined by external factors [3]. The desorption can be substantially increased by bubbling.

3. Modeling the desorption of carbon dioxide in vertical tube falling film evaporators

In the following, a model is described that allows the prediction of the CO₂ flow rates which are released from the evaporating brine in vertical tube falling film evaporators. The phase interface area, the mass transfer coefficient in falling films, and the Henry's law coefficient of CO₂ in seawater are discussed in detail.

For the description of the CO₂ release and the carbonate system in vertical tube falling film evaporators, the following assumptions are made:

- The gases nitrogen, oxygen, and argon are removed from the feed water by deaeration before entering the evaporator.
- Before entering the evaporator, the brine is preheated to its saturation temperature under such a high pressure that no gases will be released.
- The feed water is fed to the top of a tube bundle and flows down the inner walls as a thin closed liquid film. Because of the condensing steam on the outside of the tubes, part of the brine evaporates. The vapor produced flows downwards in co-current flow with the evaporating brine.
- As the driving temperature difference is very small, the evaporation takes place in the surface evaporation regime.
- The carbon dioxide released is removed continuously with the vapor so that no accumulation occurs in the gaseous phase over the brine.
- Calcium carbonate and magnesium hydroxide precipitate in negligible quantities.

3.1. The carbonate system

The carbonate system, the reaction mechanisms, the reaction rate constants, and the chemical equilibrium constants of carbonic acid in seawater have been described in detail by one of the authors [9–11]. In the following, the main features are summarized.

The carbonate system can be described by the concentrations of dissolved carbon dioxide, bicarbonate ions, carbonate ions, the pH value, the total inorganic carbon content,

$$TC = [\text{HCO}_3^-] + [\text{CO}_3^{2-}] + [\text{CO}_2], \quad (1)$$

and the total alkalinity,

$$TA = [\text{HCO}_3^-] + 2[\text{CO}_3^{2-}] + [\text{OH}^-] - [\text{H}^+]. \quad (2)$$

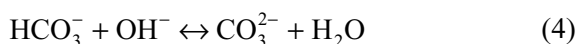
The concentration of undissociated carbonic acid H₂CO₃ is so small that it can be neglected in Eq. (1).

A combination of at least two of these six quantities is needed to characterize the carbonate system in chemical equilibrium. The remaining four quantities can be determined by applying the law of mass action with the dissociation constants of carbonic acid and water in seawater.

The hydration and dehydration of CO₂ in aqueous bicarbonate–carbonate solutions occur by two reaction mechanisms in parallel. In the pH and temperature range prevailing in desalination distillers, the alkaline reaction mechanism with the steps



and



predominates.

The rates of the reaction steps differ notably. The reaction CO₂ + OH⁻ ↔ HCO₃⁻ is relatively slow and therefore it is the rate-determining step in the alkaline reaction mechanism [9–11].

The OH⁻ ions are present in excess so that their concentrations in the boundary layer at the gas/liquid interface are not considerably changed by the reactions and can be assumed to remain constant [9–11]. The forward reaction (3) can be considered to be pseudo-first order with the rate constant

$$k_1 = k_2 C_{\text{OH}^-}, \tag{5}$$

where k_2 is the second-order rate constant of the forward reaction (3) and C_{OH^-} is the concentration of the OH⁻ ions.

3.2. Mole balances over volume elements

For the numerical model, the liquid film and the adjacent gas phase flowing down on the inside of the tube are divided into volume elements. On the one hand, the volume element must be large enough so that the residence time of the brine is higher than the reaction time and the reactions can occur in the volume element. On the other hand, the volume element must be so small that the amount of CO₂ released is lower than the amount of CO₂ that is molecularly dissolved in the volume element.

Fig. 1 shows a volume element of the falling film with the adjacent gas phase. The molar flow rate of total inorganic carbon ($\text{TC}_i \cdot \dot{m}_{\text{SW},i}$), the sum of the flow rates of CO₂ released in the preceding volume elements, and the sum of the vapor flow rates produced in the preceding volume elements enter the volume element i . A flow rate of CO₂ is released and a flow rate of vapor is produced in the volume element i . The molar flow rate of total inorganic carbon, the sum of the flow rates of CO₂ released, and the sum of the vapor flow rates produced leave the volume element i .

The total alkalinity TA and the total inorganic carbon content TC at the outlet of a volume element are calculated by means of mole balances. The total inorganic carbon content TC is affected by both the evaporation of water and the release of CO₂:

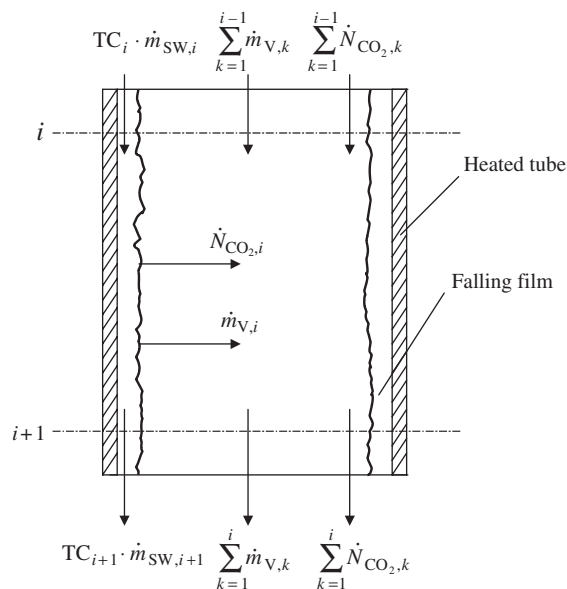


Fig. 1. Volume element in a vertical tube falling film evaporator.

$$\text{TC}_{i+1} = \frac{\text{TC} \cdot \dot{m}_{\text{SW},i} - \dot{N}_{\text{CO}_2,i}}{(\dot{m}_{\text{SW},i} - \dot{m}_{\text{V},i})}. \tag{6}$$

The desorption of CO₂ does not influence the total alkalinity. It is only changed by the evaporation of water. Thus, the total alkalinity at the outlet of element i can be obtained by

$$\text{TA}_{i+1} = \frac{\text{TA}_i \cdot \dot{m}_{\text{SW},i}}{(\dot{m}_{\text{SW},i} - \dot{m}_{\text{V},i})}. \tag{7}$$

After determining the total alkalinity and the total inorganic carbon content, the remaining quantities CO₂, HCO₃⁻, CO₃²⁻, and pH at the outlet of a volume element can be calculated by applying the law of mass action with the dissociation constants of carbonic acid and water in seawater.

3.3. Description of mass transfer with chemical reaction

The fundamentals of desorption with chemical reaction have been summarized by one of the authors [9,10].

In vertical tube falling film evaporators, the partial pressure of CO_2 in equilibrium with the bulk liquid is much smaller than the total pressure in the evaporator stages. Thus, CO_2 is considered to be released by quiescent desorption and not by bubble desorption.

For gases like SO_2 , NH_3 , and HCl that are highly soluble or react rapidly the gas phase resistance controls the mass transport. For gases that are less soluble and do not react at all or only slowly the liquid phase resistance predominates and controls the total resistance [9,10]. Since the rate-determining reaction step in the alkaline reaction mechanism is relatively slow and the solubility of CO_2 in seawater is low, it is assumed that the liquid-side mass transfer controls the desorption process.

Different models have been proposed for describing mass transfer processes at liquid/gas interfaces. These are, among others, the film model, the penetration model, and the surface renewal model. In many circumstances the difference between predictions made on the basis of the different models will be less than the uncertainties about the values of the physical quantities used in the calculation; and it is then merely a question of convenience which of the models is used [3]. Significant differences appear only when the gaseous and liquid reactants have vastly different diffusion coefficients [6,12]. The choice between the models is usually made on the basis of simplicity in describing the reacting system. For these reasons the film model has been more widely used and is applied to the CO_2 release process in vertical tube falling film evaporators.

For describing the chemical desorption process, a differential volume element of liquid at the gas/liquid phase interface is considered. A mole balance on the component i leads to the following differential equation which describes the concentration field of this component. It represents the phenomenon of simultaneous mass transport and chemical reaction:

$$\underbrace{\frac{\partial C_i}{\partial t}}_{\text{accumulation}} = D_i \underbrace{\left(\frac{\partial^2 C_i}{\partial x^2} + \frac{\partial^2 C_i}{\partial y^2} + \frac{\partial^2 C_i}{\partial z^2} \right)}_{\text{molecular transport}} - \underbrace{u_x \frac{\partial C_i}{\partial x} - u_y \frac{\partial C_i}{\partial y} - u_z \frac{\partial C_i}{\partial z}}_{\text{convective transport}} + \underbrace{r_i}_{\text{reaction}} \quad (8)$$

Here, x is the coordinate perpendicular to the phase interface, y is the coordinate in mainstream direction and z is the coordinate crosswise to it. u_x , u_y , and u_z are the velocity components in the coordinate directions, and r_i is the reaction rate.

Applying the film theory, the transient term, the terms of the convective transport as well as the molecular transport in y and z directions in Eq. (8) are dropped. Since it was found that reaction (3) is the rate-determining step in the predominating alkaline reaction mechanism, the complex system of nonlinear differential equations that describes the concentration fields of the components in the carbonate system at the gas/liquid phase interface can be reduced to a set of two linear differential equations and solved analytically (e.g. [12]).

The desorbing CO_2 flow can be expressed as

$$\dot{N}_{\text{CO}_2} = k_L^0 \cdot A_{\text{ph}} \cdot \frac{(1 + D \cdot K) \cdot (C_{\text{CO}_2, \text{B}} - C_{\text{CO}_2, \text{Ph}}^*) + D \cdot K \cdot \left(1 - \frac{1}{\cosh \left(Ha \cdot \sqrt{1 + \frac{1}{D \cdot K}} \right)} \right) \cdot \left(\frac{1}{K} \cdot C_{\text{HCO}_3, \text{B}} - C_{\text{CO}_2, \text{B}} \right)}{1 + D \cdot K \cdot \frac{\tanh \left(Ha \cdot \sqrt{1 + \frac{1}{D \cdot K}} \right)}{Ha \cdot \sqrt{1 + \frac{1}{D \cdot K}}}} \quad (9)$$

with the Hatta number

$$Ha = \frac{\sqrt{D_{CO_2,SW} \cdot k_1}}{k_L^0}, \tag{10}$$

the equilibrium constant K of reaction (3) considered to be pseudo-first order:

$$K = \frac{K_1^{SW}}{K_w^{SW}} \cdot [OH^-]^{eq}, \tag{11}$$

and the ratio of the diffusion coefficients of HCO_3^- and CO_2 in the brine

$$D = \frac{D_{HCO_3^-,SW}}{D_{CO_2,SW}}. \tag{12}$$

According to Danckwerts and Sharma [13] it can be assumed for technical purposes that the diffusion coefficients of HCO_3^- and CO_2 have similar values, i.e. $D \approx 1$.

The diffusion coefficient of CO_2 in seawater $D_{CO_2,SW}$ is described in Refs. [10,11]. The CO_2 concentration in the bulk of the liquid $C_{CO_2,B}$ is calculated by applying the law of mass action with the dissociation constants of carbonic acid and water in seawater. The reaction rate constant k_1 and the dissociation constants K_1^{SW} and K_w^{SW} were discussed in detail in Refs. [9–11].

In order to calculate the molar flow rate of CO_2 given in Eq. (9), the mass transfer coefficient k_L^0 , the phase interface area A_{ph} , the CO_2 concentration at the phase interface $C_{CO_2,Ph}$, and the Henry's law coefficient $H_{CO_2,SW}$ are required. The determination of these quantities will be discussed in the following sections.

3.4. The phase interface area

The phase interface area for CO_2 release consists of the surface area of the brine being distributed onto the tube bundle, the free surface area of the falling films in the vertical tubes, and the surface area of the concentrated brine collected at the bottom of the evaporator. As a first

approach, the main focus is put on the free surface area of the falling film.

The free surface area of the falling film in one tube is given by

$$A_{Ph,tube} = \pi \cdot (d_i - 2 \cdot s) \cdot L_T, \tag{13}$$

where L_T is the length of the tube and s is the liquid film thickness.

From optical measurements Brauer [14] found that the phase interface enlargement of falling films in vertical tubes by surface waves is smaller than 3%. Thus, the enlargement of the phase interface area by waves is neglected.

The flow of falling films in vertical tubes can be divided into laminar, laminar-wavy, transitional, and turbulent flow. The characteristic number for the flow regimes is the film Reynolds number given by

$$Re_F = \frac{\dot{m}_{SW}}{\pi \cdot d_i \cdot \eta}. \tag{14}$$

According to ESDU Report 98010 [15] the flow regimes can be subdivided as follows:

laminar:	$Re_F < 8$
laminar-wavy:	$8 \leq Re_F < 400$
transitional:	$400 \leq Re_F < 800$
turbulent:	$800 \leq Re_F$.

According to Nusselt [14] the film thickness for laminar flow can be expressed as

$$s_{lam} = \left(\frac{3\nu^2}{g} \right)^{1/3} Re_F^{1/3}. \tag{15}$$

For the laminar-wavy flow regime Kapitza [16] proposed

$$s_{wavy} = \left(\frac{2.4\nu^2}{g} \right)^{1/3} Re_F^{1/3}. \tag{16}$$

In the transient and turbulent flow regime a correlation given by Brauer [14] can be applied:

$$s_{\text{turb}} = 0.302 \left(\frac{3\nu^2}{g} \right)^{1/3} Re_F^{8/15}. \quad (17)$$

3.5. The mass transfer coefficient in falling films

The mass transfer coefficient can be calculated from the Sherwood number with

$$Sh = \frac{k_L^0 \cdot \ell}{D_{ij}}, \quad (18)$$

where ℓ is the characteristic length

$$\ell = 3 \sqrt[3]{\frac{\nu^2}{g}}. \quad (19)$$

From the various correlations [17–20] available for Sherwood numbers describing mass transfer between falling films and gases we have chosen the one proposed by Mayinger [18] because it is based on the measurement results from various researchers and it is valid for a wide range of Reynolds and Schmidt numbers.

The empirical correlations given by Mayinger [18] are valid for falling films in the laminar-wavy, transition and turbulent flow regime:

$$Sh = 2.24 \times 10^{-2} \cdot Re_F^{0.8} \cdot Sc^{0.5} \text{ for} \\ 12 \leq Re_F \leq 70 \text{ and } Sc \geq \frac{2.32 \times 10^4}{Re_F^{1.6}}, \quad (20)$$

$$Sh = 8.0 \times 10^{-2} \cdot Re_F^{0.5} \cdot Sc^{0.5} \text{ for} \\ 70 \leq Re_F \leq 400 \text{ and } Sc \geq \frac{1.82 \times 10^3}{Re_F}, \quad (21)$$

$$Sh = 8.9 \times 10^{-4} \cdot Re_F^{1.25} \cdot Sc^{0.5} \text{ for} \\ Re_F \geq 400 \text{ and } Sc \geq \frac{1.47 \times 10^7}{Re_F^{2.5}}, \quad (22)$$

where Re_F is the film Reynolds number given in Eq. (14), and Sc is the Schmidt number

$$Sc = \frac{\nu}{D_{ij}}. \quad (23)$$

3.6. Henry's law coefficient

Since the concentration of CO_2 in seawater is small enough to fulfill the required condition of high dilution, the solubility may be described by using Henry's law:

$$C_{\text{CO}_2} = H_{\text{CO}_2, \text{sw}} \cdot p_{\text{CO}_2}, \quad (24)$$

where C_{CO_2} is the concentration of the dissolved CO_2 in seawater, p_{CO_2} is the partial pressure of CO_2 in the gas phase, and $H_{\text{CO}_2, \text{sw}}$ is Henry's law coefficient of CO_2 in seawater.

As Henry's law only describes the physical equilibrium between a liquid and a gaseous phase, it may only be applied to the fraction of carbon dioxide that is physically dissolved and not chemically bound. Henry's law coefficient depends on the solvent and the gas, the total pressure, the temperature, the ionic strength of the solution, and the concentrations of other dissolved gases. The dependency on the total pressure and on the concentration of other dissolved gases may be neglected in this case as the total pressure is much lower than 5 bar [21].

By adding salts to a solution the solubility of gases is lowered. Danckwerts [3] proposed to determine Henry's law coefficient in the salt solution by relating it to Henry's law coefficient in water at the same temperature as originally described by Sechenov [22]:

$$\log \left(\frac{H_{\text{G,W}}}{H_{\text{G,SW}}} \right) = h \cdot I, \quad (25)$$

where h is the sum of ion and gas specific parameters

$$h = h_+ + h_- + h_G \quad (26)$$

and I is the ionic strength of a solution which is defined as

$$I = \frac{1}{2} \sum_i z_i^2 m_i \quad (27)$$

with the charge of the ion z_i and the molality of the ion m_i .

Millero [23] proposed a correlation between the ionic strength and the salinity of seawater:

$$I = \frac{19.92 S}{1000 - 1.005 S} \quad (28)$$

with S in g/kg and I in mol/kg.

Ion and gas specific parameters were experimentally determined for various ions and gases (e.g. [24,25]). It is assumed that the temperature dependence of h is confined to the change in h_G , but there are only very few data available in literature. The ion specific parameters are considered to be independent of temperature.

As the ionic strength of seawater is dominated by sodium chloride to an extent of 73%, only the ion specific parameters of Na^+ and Cl^- are taken into account. The temperature dependence of the gas specific parameter of CO_2 is neglected because of a lack of data for the relevant temperature range. Onda et al. [25] proposed the following values for the gas specific parameter at 40°C and the ion specific parameters:

$$\begin{aligned} h_{\text{Na}^+} &= -0.0183 \text{ L/mol}, & h_{\text{Cl}^-} &= 0.3416 \text{ L/mol}, \\ h_{\text{CO}_2} &= -0.2327 \text{ L/mol}. \end{aligned} \quad (29)$$

Henry’s law coefficient of CO_2 in pure water is determined with a correlation given by Yaws et al. [26], which is valid for temperatures up to 80°C:

$$\begin{aligned} \log H_{\text{CO}_2, \text{w}} &= 69.4237 - \frac{3796.46}{T} \\ &- 21.6694 \cdot \log T + 0.000478857 \cdot T, \end{aligned} \quad (30)$$

where $H_{\text{CO}_2, \text{w}}$ is in atm per mole fraction and T is in K.

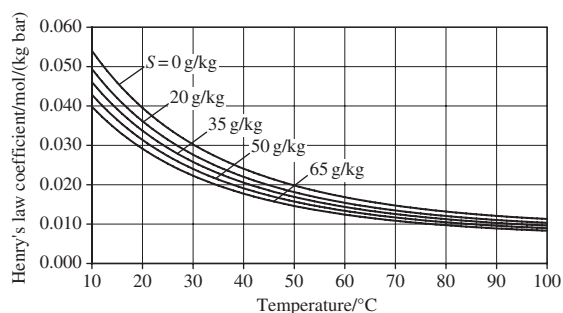


Fig. 2. Henry’s law coefficient of CO_2 in pure water ($S=0$ g/kg) and seawater as a function of temperature at different salinities.

The solubility of CO_2 in seawater was experimentally determined up to 40°C and $S=40$ g/kg by Li and Tsui [27], Murray and Riley [28] and Weiss [29]. Weiss proposed a correlation that is based on his own measured values and those of Murray and Riley. Since the extrapolation of this correlation to higher temperatures and salinities does not give reliable results, it is proposed here to determine Henry’s law coefficient of CO_2 in seawater with Eq. (25) using Eq. (30) for Henry’s law coefficient in pure water.

Fig. 2 shows Henry’s law coefficient of CO_2 in pure water and in seawater as a function of temperature at different salinities. The correlation for Henry’s law coefficient in pure water (Eq. (30)) given by Yaws et al. [26] was extrapolated to temperatures above 80°C. The Henry’s law coefficient of CO_2 decreases with increasing temperature in the temperature range depicted. Henry’s law coefficient also decreases with increasing salinity.

3.7. The CO_2 concentration at the phase interface

For calculating the CO_2 concentration at the phase interface, the following assumptions are made:

- The resistance at the phase interface itself is usually negligible and physical equilibrium may be assumed to prevail [30].

- Both for NC gases and water vapor the deviation from the ideal gas equation of state is negligible at the low pressures in falling film evaporators.

The CO₂ concentration in the brine at the phase interface is determined by applying Henry's law as given by Eq. (24).

The partial pressure of CO₂ $p_{\text{CO}_2,i}$ in the gas phase over the brine surface in the volume element i is given by

$$p_{\text{CO}_2,i} = \frac{\dot{N}_{\text{CO}_2,i}}{\dot{N}_{\text{V},i}} \cdot p_{\text{V},i} = \frac{\dot{N}_{\text{CO}_2,i}}{\dot{N}_{\text{V},i}} \times (p_{\text{tot}} - p_{\text{CO}_2,i} - p_{\text{N}_2,i} - p_{\text{O}_2,i} - p_{\text{Ar},i}) \quad (31)$$

with $\dot{N}_{\text{CO}_2,i}$ as the molar flow rate of CO₂ in the volume element, $\dot{N}_{\text{V},i}$ as the molar flow rate of vapor, $p_{\text{V},i}$ as the partial pressure of vapor, p_{tot} as the total pressure, and $p_{\text{N}_2,i}$, $p_{\text{O}_2,i}$ and $p_{\text{Ar},i}$ as the partial pressures of N₂, O₂ and Ar.

When applying Henry's law the CO₂ phase interface concentration can be expressed as

$$C_{\text{CO}_2,\text{Ph},i} = H_{\text{CO}_2,\text{SW},i} \times \frac{\dot{N}_{\text{CO}_2,i} (p_{\text{tot}} - p_{\text{N}_2,i} - p_{\text{O}_2,i} - p_{\text{Ar},i})}{\dot{N}_{\text{V},i} + \dot{N}_{\text{CO}_2,i}} \quad (32)$$

Assuming that the feed water is deaerated, the partial pressures of N₂, O₂ and Ar can be neglected in Eq. (32).

4. Simulation of the CO₂ release in vertical tube falling film evaporators

Currently, experiments are being carried out in a falling film evaporator with a single vertical tube in order to verify the model. To show the capabilities of the developed model it was applied to this falling film evaporator.

The main part of the reference evaporator is a 2.5 m long stainless steel tube with an inner diameter of $d_i = 36$ mm. The tube is concentrically surrounded by a shell where heating steam condenses on the outside of the vertical tube providing a constant heat flux of 20 kW/m². The mass flow rate of the feed water at the top of the tube is assumed to be 101.8 kg/h which leads to a wetting rate of $\Gamma = 0.25$ kg/(s m). For calculating the CO₂ release and the carbonate system, the 2.5 m long tube was divided into 70 volume elements.

Depending on the Hatta number Ha and the chemical equilibrium constant K , a number of asymptotic solutions of Eq. (9) can be found [3,4]. The desorption regime strongly depends on the process parameters such as evaporation temperature, wetting rate, and seawater salinity. In the following, it is discussed in which desorption regime the CO₂ release process takes place and whether the mass transfer is enhanced by the chemical reactions.

For a wetting rate of $\Gamma = 0.25$ kg/(s m), a seawater salinity of $S = 35$ g/kg, a seawater pH of 8.15, and evaporation temperatures below around 50°C, the Hatta number is lower than 0.3, i.e., the rate-determining reaction is slower than the mass transfer. The desorption takes place in the so-called slow reaction regime. The reactions only occur in the bulk flow, not in the boundary layer at the phase interface. The mass transfer in the boundary layer is not enhanced by the reactions.

At evaporation temperatures above around 50°C, desorption takes place in the transition regime between slow and fast reactions. Mass transfer and chemical reactions simultaneously take place in the boundary layer. The bulk of the brine is in chemical equilibrium. In the transition regime between slow and fast reactions, the chemical rate constant k_1 becomes more important and the mass transfer coefficient k_L^0 becomes less important. Mass transfer is slightly enhanced by the reaction.

At high evaporation temperatures above 100°C, low wetting rates, and high seawater salinities, desorption takes place in the fast reaction regime. In the fast reaction regime, the influence of the mass transfer coefficient k_L^0 on the desorption rate is negligible. Mass transfer is enhanced by the reactions. The CO₂ release rates, however, are low because the interfacial area and the concentration difference of CO₂ between bulk and phase interface, the driving force for mass transfer, are small.

Fig. 3 shows the accumulated CO₂ release rate along the flow path of the falling film in the reference evaporator for different evaporation temperatures. At a constant wetting rate of $\Gamma = 0.25$ kg/(s m) and an evaporation temperature of 40°C laminar-wavy flow occurs, at 70°C the flow is in the transition regime, and at 100°C it is turbulent.

In seawater with $S = 35$ g/kg, pH = 8.15, and TA = 0.0023 mol/kg at $t_{sw} = 25^\circ\text{C}$, 0.415 mg/kg CO₂ are molecularly dissolved. If only the CO₂ that is molecularly dissolved in seawater was released, the release rate would be 0.0422 g/h. As shown in Fig. 3, the release rates are considerably higher, because the chemical reactions produce new CO₂ that is subsequently released. The reactions provide a certain concentration of

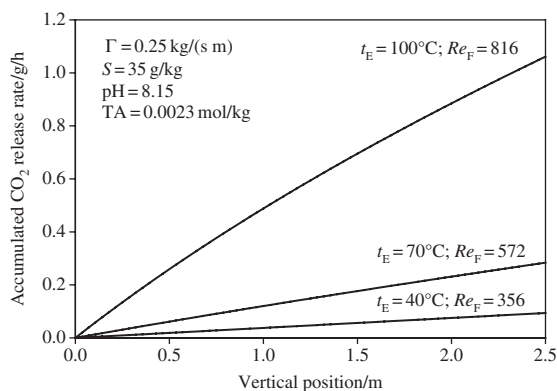


Fig. 3. Accumulated CO₂ release rate along the flow path of the falling film in the reference evaporator for different evaporation temperatures t_E .

the molecularly dissolved gas in the bulk of the liquid and hence a certain driving force for the mass transfer. At an evaporation temperature of 40°C about 1% of the total inorganic carbon content entering the evaporator with the feed water is released as CO₂, at an evaporation temperature of 100°C about 12% of the total inorganic carbon content is released.

The CO₂ release rate decreases along the flow path of the falling film. The total inorganic carbon content decreases and the pH increases because of the CO₂ release. Thus, the CO₂ concentration in the brine bulk decreases. The CO₂ concentration at the phase interface decreases because the brine is evaporated and the salinity rises. The overall effect is that the difference between CO₂ concentration in the bulk and at the phase interface, the driving force for mass transfer, decreases.

The CO₂ release significantly increases with increasing evaporation temperature because of the following reasons:

- The mass transfer coefficient increases with rising temperature.
- The difference between CO₂ concentration in the bulk and at the phase interface, the driving force for mass transfer, increases with temperature.
- At temperatures higher than around 50°C the mass transfer is slightly enhanced by the chemical reactions.

Fig. 4 shows the influence of the evaporation temperature on CO₂ release for different salinities of the feed water. The CO₂ release increases with rising evaporation temperature on progressive scale because of the reasons mentioned above. Furthermore, the CO₂ release increases with increasing salinity of the feed water. This can be attributed to the following reasons:

- The total alkalinity TA increases with increasing salinity. At constant pH the total inorganic carbon TC increases. Thus, the CO₂ concentration in the bulk flow increases.

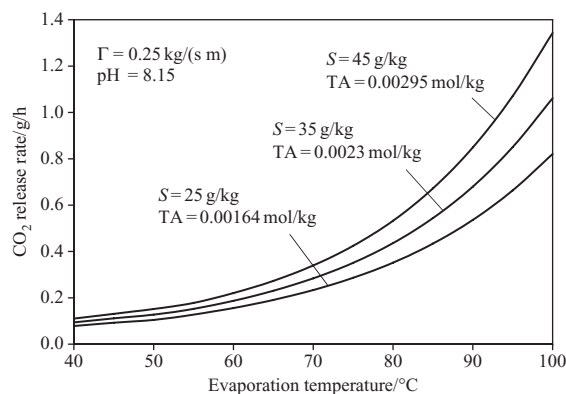


Fig. 4. The influence of the evaporation temperature on the CO_2 release in the reference evaporator for different salinities of the feed water.

- The solubility of CO_2 decreases with increasing salinity. Thus, the CO_2 concentration in the brine at the phase interface decreases. Since the concentration in the bulk increases and the concentration at the phase interface decreases, the driving concentration difference for mass transfer increases.

The influence of the pH value of the feed water on the CO_2 release is shown in Fig. 5. The CO_2 release increases with decreasing pH. At

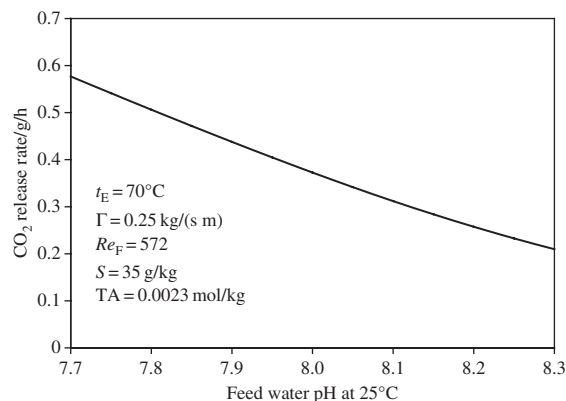


Fig. 5. The influence of the feed water pH on the CO_2 release in the reference evaporator.

low seawater pH values more CO_2 dissolved in seawater and reacted to carbonic acid which dissociated into HCO_3^- and CO_3^{2-} ions. Therefore, the total inorganic carbon content is higher. Moreover, the fraction of the total inorganic carbon content that is present as molecular CO_2 is higher at low pH values. The CO_2 concentration in the bulk flow and thus the driving concentration difference for mass transfer increase with decreasing pH value of the seawater. Therefore, more CO_2 is released.

5. Conclusion

A model has been developed for the prediction of CO_2 release rates in vertical tube falling film evaporators. In addition to the release rates the model allows for calculation of the HCO_3^- , CO_3^{2-} , CO_2 , H^+ , and OH^- concentrations in the carbonate system of the brine. The desorption of CO_2 was described as a problem of mass transfer coupled with chemical reaction. The phase interface area, the mass transfer coefficient, and Henry's law coefficient of CO_2 in seawater were presented in detail.

Given the main dimensions of the evaporator, the operating data and the measurable pH and total alkalinity of seawater, the CO_2 release rates as well as the HCO_3^- , CO_3^{2-} , CO_2 , H^+ , and OH^- concentrations in the brine can be calculated along the flow path of the falling film.

In order to show the capabilities of the model, it was applied to a falling film evaporator with a single vertical tube. The release rates of CO_2 were simulated at various evaporation temperatures, seawater salinities, and pH values. The CO_2 release rates along the flow path of the falling film were shown. CO_2 release increases with increasing evaporation temperature and seawater salinity and decreasing pH of the seawater.

Currently, the CO_2 release is being measured in a vertical tube falling film evaporator test rig in order to verify and improve the model.

Nomenclature

C_i	concentration of the component i , mol/m ³
D	ratio of diffusion coefficients
D_{ij}	binary diffusion coefficient, m ² /s
d_i	inner diameter, m
g	gravitational acceleration, m/s ²
$H_{i,j}$	Henry's law coefficient, mol/(m ³ bar)
Ha	Hatta number
h	sum of gas and ion specific parameters, L/mol
h_G	gas specific parameter, L/mol
h_+	ion specific parameter for cations, L/mol
h_-	ion specific parameter for anions, L/mol
I	ionic strength, mol/kg
$[i]$	concentration of the component i , mol/kg solution
K	chemical equilibrium constant of the pseudo-first order reaction
K_1^{SW}	first dissociation constant of carbonic acid in seawater on the basis mol/kg solution
K_W^{SW}	dissociation constant of water in seawater on the basis mol/kg solution
k_L^0	mass transfer coefficient in the liquid phase without chemical reaction, m/s
k_1	first-order rate constant of the forward reaction, 1/s
k_2	second-order rate constant of the forward reaction, m ³ /(mol s)
L_T	tube length, m
l	characteristic length, m
\dot{m}	mass flow rate, kg/s
m_i	molality, mol/kg
\dot{N}	molar flow rate, mol/s
p	pressure, bar
p_i	partial pressure, bar
Re_F	film Reynolds number
r_i	reaction rate of the component i , mol/(m ³ s)
S	salinity, g/kg
s	film thickness, m
Sc	Schmidt number
Sh	Sherwood number

T	temperature, K
t	temperature, °C
TA	total alkalinity, mol/kg
TC	total inorganic carbon content, mol/kg
u	flow velocity
z_i	charge of the ion i

Greek symbols

Γ	wetting rate, kg/(s m)
η	dynamic viscosity, Pa s
ν	kinematic viscosity, m ² /s
ρ	density, kg/m ³
σ	surface tension, N/m

Indices

Ar	argon
B	bulk
CO ₂	carbon dioxide
E	evaporation
eq	chemical equilibrium
G	gas
i	component, volume element
lam	laminar
N ₂	nitrogen
O ₂	oxygen
Ph	phase interface
SW	seawater
tot	total
turb	turbulent
V	vapor
W	water
wavy	laminar-wavy
*	physical equilibrium

References

- [1] J.W. Vermey, Large scale application of vertical tube mechanical vapour compression technology, Proc. IDA World Congress on Desalination and Water Reuse, Gran Canaria, 2007, submitted for publication.
- [2] Y.T. Shah and M.M. Sharma, Desorption with or without chemical reaction, Trans. Inst. Chem. Eng., 54 (1967) 1–41.
- [3] P.V. Danckwerts, Gas–Liquid Reactions, McGraw-Hill, New York, 1970.

- [4] G. Astarita, Mass Transfer with Chemical Reaction, Elsevier, Amsterdam, 1967.
- [5] G. Astarita, General mathematical layout of multiphase systems, NATO ASI Series, Series E, 72 (1) (1983) 17–36.
- [6] S. Carra and M. Morbidelli, Gas–liquid reactors, in: J.J. Carberry and A. Varma (Eds.), Chemical Reaction and Reactor Engineering, Marcel Dekker, New York, 1987, pp. 545–666.
- [7] H. Ishikawa, T. Miki, M. Okamoto and H. Hikita, Gas desorption from liquids: mass transfer and drag coefficients for single bubbles in free rise through newtonian liquids, Chem. Eng. Sci., 41 (1986) 2309–2319.
- [8] W. Pasiuk-Bronikowska and K.J. Rudzinski, Gas desorption from liquids, Chem. Eng. Sci., 36 (1981) 1153–1159.
- [9] H. Glade, Chemical reaction kinetics and mass transfer phenomena controlling the release of CO₂ in MSF distillers, Proc. IDA World Congress on Desalination and Water Reuse, San Diego, USA, Vol. 1, 1999, pp. 375–388.
- [10] H. Glade, Transport und Reaktion von Kohlendioxid in Entspannungsverdampfern zur Meerwasserentsalzung, Ph.D. Thesis, University of Bremen, 2001, VDI Fortschritt-Berichte, Series 3, No. 699, VDI Verlag, Düsseldorf, 2001.
- [11] A.E. Al-Rawajfeh, H. Glade and J. Ulrich, CO₂ release in multiple-effect distillers controlled by mass transfer with chemical reaction, Desalination, 156 (2003) 109–123.
- [12] C.-J. Huang and C.-H. Kuo, Mathematical models for mass transfer accompanied by reversible chemical reaction, AIChE J., 11 (1965) 901–910.
- [13] P.V. Danckwerts and M.M. Sharma, The absorption of carbon dioxide into solutions of alkalis and amines (with some notes on hydrogen sulphide and carbonyl sulphide), Chem. Eng., (1966) 244–280.
- [14] H. Brauer, Grundlagen der Ein- und Mehrphasenströmung, Verlag Sauerländer, Aarau, 1971.
- [15] ESDU, Falling Film Evaporation in Vertical Tubes, ESDU Report 98010, 1998.
- [16] P.L. Kapitza, Collected Papers of P.L. Kapitza, Volume II, Chapter 43: Wave Flow of Thin Layers of a Viscous Fluid, Pergamon Press, Oxford, 1965.
- [17] H. Brauer and D. Mewes, Stoffaustausch einschließlich chemischer Reaktion, Verlag Sauerländer, Aarau, 1971.
- [18] F. Mayinger, Strömung und Wärmeübergang in Flüssigkeitsgemischen, Springer Verlag, Berlin, 1982.
- [19] S. Kamei and J. Oishi, Mass and heat transfer in a falling liquid film of wetted wall tower, Memoirs of the Faculty of Engineering Kyoto, 1955, pp. 277–289.
- [20] H. Thiele, Absorption im laminaren Film mit ebener Oberfläche, Ph.D. Thesis, Technische Universität Berlin, Germany, 1966.
- [21] J. Falbe (Ed.), Römpf Chemie Lexikon, 10th edn., Georg Thieme Verlag, Stuttgart, 1997.
- [22] M. Sechenov, Über die Konstitution der Salzlösungen auf Grund ihres Verhaltens zu Kohlensäure, Z. Phys. Chem., 4 (1889) 117–125.
- [23] F.J. Millero, Thermodynamics of the carbon dioxide system in the ocean, Geochim. Cosmochim. Acta, 59 (1995) 661–677.
- [24] C. Hermann, I. Dewes and A. Schumpe, The estimation of gas solubilities in salt solutions, Chem. Eng. Sci., 50 (1995) 1673–1675.
- [25] K. Onda, E. Sada, T. Kobayashi, S. Kito and K. Ito, Salting-out parameters of gas solubility in aqueous salt solutions, Chem. Eng. Jpn., 3 (1970) 18–24.
- [26] C.L. Yaws, J.R. Hopper, X. Wang, A.K. Rathinsamy and R.W. Pike, Calculating solubility & Henry's law constants for gases in water, Chem. Eng., 106 (1999) 102–105.
- [27] Y.H. Li and T.F. Tsui, The solubility of CO₂ in water and seawater, J. Geophys. Res., 76 (1971) 4203–4207.
- [28] C.N. Murray and J.P. Riley, The solubility of gases in distilled water and seawater. IV. Carbon dioxide, Deep-Sea Res., 18 (1971) 533–541.
- [29] R.F. Weiss, Carbon dioxide in water and seawater: the solubility of a non-ideal gas, Mar. Chem., 2 (1974) 203–215.
- [30] H.D. Baehr and K. Stephan, Wärme- und Stoffübertragung, 2nd edn., Springer-Verlag, Berlin, 1996.